



Deposited via The University of Leeds.

White Rose Research Online URL for this paper:

<https://eprints.whiterose.ac.uk/id/eprint/141849/>

Version: Accepted Version

---

**Article:**

Luhaib, SWO, Bakr, MS, Hunter, IC et al. (2020) Compact Triple-Mode Microwave Dielectric Resonator Filters. *International Journal of Electronics*, 8 (2). pp. 194-204. ISSN: 0020-7217

<https://doi.org/10.1080/00207217.2019.1582714>

---

© 2019 Informa UK Ltd, trading as Taylor & Francis Group. This is an author produced version of a paper published in *International Journal of Electronics Letters*. Uploaded in accordance with the publisher's self-archiving policy.

**Reuse**

Items deposited in White Rose Research Online are protected by copyright, with all rights reserved unless indicated otherwise. They may be downloaded and/or printed for private study, or other acts as permitted by national copyright laws. The publisher or other rights holders may allow further reproduction and re-use of the full text version. This is indicated by the licence information on the White Rose Research Online record for the item.

**Takedown**

If you consider content in White Rose Research Online to be in breach of UK law, please notify us by emailing [eprints@whiterose.ac.uk](mailto:eprints@whiterose.ac.uk) including the URL of the record and the reason for the withdrawal request.



## Compact Triple-Mode Microwave Dielectric Resonator Filters

|  |  |
|--|--|
| Journal:   | <i>International Journal of Electronics</i>  |
| Manuscript ID  | TETN-2018-1132   |
| Manuscript Type:   | International Journal of Electronics Letters (2500 word limit)   |
| Date Submitted by the Author:  | 12-Nov-2018  |
| Complete List of Authors:  | Luhaib, Saad; University of Leeds School of Electronic and Electrical Engineering, Pollard Insitute; College of Engineering, Electrical Engineering<br>Bakr, Mustafa; University of Leeds School of Electronic and Electrical Engineering, Pollard Insitute<br>Hunter, Ian; University of Leeds School of Electronic and Electrical Engineering, Pollard Insitute<br>Somjit , Nutapong; University of Leeds School of Electronic and Electrical Engineering, Pollard Institute |
| Keywords:  | Triple-mode, Dielectric Resonator Filters, Microwave Bandpass Filters, Compact Filters, Base Station Applications  |
| <p>Note: The following files were submitted by the author for peer review, but cannot be converted to PDF. You must view these files (e.g. movies) online.</p> <p>Triple-Mode _JOURnal.rar</p> |  |

SCHOLARONE™  
Manuscripts

## ARTICLE TEMPLATE

**Compact Triple-Mode Microwave Dielectric Resonator Filters**Saad W. O. Luhaib<sup>a,b</sup>, Mustafa S. Bakr<sup>a</sup>, Nutapong Somjit<sup>a</sup> and Ian C. Hunter<sup>a</sup><sup>a</sup>School of Electronic and Electrical Engineering, University of Leeds, Leeds, UK;<sup>b</sup>Electrical Engineering Department, University of Mosul, Mosul, Iraq**ARTICLE HISTORY**

Compiled November 12, 2018

**Abstract**

This paper presents a novel and compact triple-mode dielectric resonator (DR) band-pass filter (BPF) based on a single waveguide cavity. A triple-mode resonator can be achieved by pairing the degenerate  $EH_{11}$  modes with a  $TM_{01\delta}$  mode. The DR structure is composed of two slitted pieces of dielectric pucks that are placed in the middle of a cylindrical metallic cavity. The resonator offers a size reduction ratio of about 15.6% compared with equivalent air-filled coaxial filters. A coaxial probe is used to excite the degenerate  $EH_{11}$  modes while the  $TM_{01}$  mode is excited using a vertical hole etched in the ceramic pucks. Finally, a 3<sup>rd</sup> order generalised Chebyshev BPF is simulated using HFSS software. The filter has finite transmission zeros (TZ) on the high or low side of the passband.

**KEYWORDS**

Triple-mode dielectric resonator, Bandpass filter, single cavity, finite transmission zeros.

**1. Introduction**

The rapid growth of mobile communications demands the design of compact RF front-ends. Microwave filters are essential components enabling efficient use of the scarce RF spectrum (Hunter et al., 2002). Dielectric resonators have been widely used in cellular base stations to design high performance and compact size filters and diplexers (Luhaib et al., 2018). However, the size of dielectric resonator filters are still large. Multi-resonances have been used in dielectric resonator filters to enable further size and mass reduction (Bakr et al., 2016b,1). In 1982, Fiedziuszko proposed the dual  $HE_{11}$  dielectric resonator filters where  $EH_{11}$  is not the fundamental mode (Fiedziuszko, 1982). A  $TE_{01}$  mode dielectric resonator filters for wireless base stations were proposed in which a dielectric puck was suspended in the middle of a metallic cavity (Liang and Blair, 1998). The aforementioned modes can be used to design triple mode resonators. However, those resonators do not operate with their fundamental resonance and thus no significant volume reduction is obtainable compared with the triply degenerate  $TE_{01}$  mode resonator proposed in (Bakr et al., 2016a,1,1; Walker and Hunter, 2002). This paper proposes the design of novel compact triple-mode dielectric resonator filters where the degenerate  $EH_{11}$  mode and the single  $TE_{01}$  mode are the fundamental resonance with high Q-factor. The triple-mode has been achieved at the fundamental

---

CONTACT Saad W. O. Luhaib. Email: elswol@leeds.ac.uk , saadw1981@gmail.com

resonance by mirroring two dielectric pucks in the middle of a metallic cavity. The filter offers a high volume reduction ratio compared with designs using similar techniques. A design example of three-pole bandpass filter with finite transmission zeros on either side is presented to validate the proposed approach.

## 2. Triple-Mode Resonator Cavity

Figure 1 depicts the configuration of the triple-mode dielectric resonator. It consists of two pieces of dielectric pucks that are suspended in the middle of a cylindrical metallic cavity.  $D_{res}$  and  $L_{res}$  are the diameter and length of the DR respectively while  $D_{cav}$  and  $L_{cav}$  are the diameter and length of the metallic cavity.  $t_{rg}$ ,  $t_g$  are the gaps between the ceramic pucks and the cavity side wall. The ceramic material used in this work is barium titanate with a relative permittivity of 43 and loss tangent of  $4 \times 10^{-5}$ . The metallic cylindrical cavity is made from copper with conductivity of  $4 \times 10^7$  S/m. A finite element method solver (HFSS) has been used to calculate the resonant frequency and unloaded Q factors ( $Q_u$ ) of the proposed resonator. Table 1 shows the calculated resonant frequencies, and  $Q_u$  for the first five modes. From the column UNP, the triple-mode was formed by intersecting the resonant frequencies of the degenerate  $EH_{11}$  mode with the  $TE_{01\delta}$  mode at a resonant frequency of 1.96 GHz. The dimensions of the resonator at this frequency were as follow;  $D_{cav}=36$  mm,  $D_{res}=32$ ,  $L_{cav}=25$  mm,  $L_{res}=10$  mm and  $t_{rg}= 2$ mm. A Parametric study has been applied to show the effect of the cavity and DR dimensions, and spacing gaps on the  $f_r$ ,  $Q_u$  and the spurious-free window. Figure 2 shows the resonant frequencies as a function of the gap between the ceramic pucks ( $t_{rg}$ ). It was observed that the dominant mode is the  $TE_{01\delta}$  for  $t_{rg} < 1.75$  mm where the second mode is the degenerate  $EH_{11}$ . As  $t_{rg}$  increased,  $EH_{11}$  is nearly unaffected. However,  $TE_{01}$  and  $TM_{01}$  modes increased linearly. At  $t_{rg}=1.75$  mm, the triple-mode was achieved. The spurious-free window is about 400 MHz, which offers good suppression in multi-mode dielectric resonator filters. The gap between the dielectric pieces and the cavity side walls were defined as 2 mm. The gap between the top and bottom faces of the dielectric resonators and the cavity walls was defined as 1.5 mm. The reduction volume ratio is about 15.6% compared with an air-filled coaxial filter at  $\sqrt{\epsilon_r}Z_0$  equal to  $77 \Omega$ .

The E- and H-fields of the first three resonances are studied at the operating resonant frequency of 1.95 GHz as shown in Figure 3. It can be seen that the E-fields of the degenerate  $EH_{11}$  mode are mainly concentrated in the gaps between the dielectric pucks and the side walls of the cavity. It is interesting to see that the E-field of the  $TE_{01\delta}$  mode varies as a function of  $\theta$  and is concentrated in the middle of the metallic cavity. The maximum H-field was in the middle of each dielectric pieces for the degenerate  $EH_{11}$  mode. The field patterns give us a good indication to what is the most appropriate method to couple this cavity, which is by exciting the E field in this case. The distance between the dielectric puck and the wall cavity is small. Therefore, it is difficult to excite the proposed resonator from the side-wall. Instead, the excitation probes are positioned from the top or bottom of the cavity as shown in Figure 4. Longitudinal grooves are etched through the ceramic pucks to facilitate the required external couplings from input to resonators. The dimensions of the rectangular grooves are defined in Figure 4 as  $L_i$ ,  $W_i$ , and  $L_{res}$ . The optimised dimensions are shown in Table 1.

The tuning mechanism must provide independent control of each of the modes. However, this is a daunting task in triple-mode dielectric resonator filters as one tuning

element creates unwanted coupling between modes; thus, break the triple degeneracy of the resonator. The next section will discuss the coupling mechanism of the proposed triple-mode dielectric resonator and constitute a bandpass filter response.

### 3. The Coupling Mechanism

As displayed in the field patterns shown in Figure 3, the best way to couple the triple-mode DR is by inserting the excitation probes from the top of the metallic cavity. Figure 4 presents the coupling structure for the proposed triple-mode DR filter. The group delay method has been applied to calculate the external coupling required (Hong, 2000) as shown in equation 1

$$Q_e = 0.5\pi f_0 \tau_d \quad (1)$$

where  $f_0$  is the resonant frequency and  $\tau_d$  is the group delay at  $f_0$ . Figure 5 illustrates the external Q-factor against the length of the probe ( $L_{fh}$ ) where the diameter of the copper probe ( $d_f$ ) is equal to 2 mm. It can be seen that the  $Q_e$  is rapidly decreased when  $L_{fh}$  increases varying between 5 mm to 15 mm. However, the  $Q_e$  gradually decreased for  $L_{fh} > 15$  mm. The resonant frequencies of the modes can be affected by the variation of  $L_{fh}$ , as provided in Figure 6. It was observed that, when  $L_{fh}$  increased, the  $EH_{11}$  dual-mode decreased while the  $TE_{01\delta}$  remained constant. From 8 mm, the  $EH_{11}$  dual-mode started to separate from each other and coupling sets between them.

Figure 7 shows the effect of introducing a through hole in the dielectric puck at an angle of  $45^\circ$  with respect to  $EH_{11}^-$  on the resonant frequencies. The diameter of the through hole was defined as ( $D_{hr}$ ) which is equal to 4 mm. The  $TE_{01\delta}$  increased to about 70 MHz when the distance between the centre of the DR and through hole ( $X_r$ ) varied between 0 to 9 mm. The resonant frequency of the  $HE_{11}$  mode decreased by 30 MHz for the same range of  $X_r$ . The effect of having tuning screws through the vertical through hole and from the side wall of the metallic cavity has been investigated. Figure 8 shows the relationship between the resonant frequencies for the triple resonances and the length of the tuning screw ( $L_{TT}$ ) that is located in the through hole. The screw diameter is defined as 4 mm while the  $X_r$  and  $D_{hr}$  are equal to 5 mm. The resonant frequency of the  $EH_{11}^-$  mode increased to about 15 MHz and the  $EH_{11}^+$  mode decreased to about 40 MHz while the  $TE_{01\delta}$  mode was slightly increased. The frequency difference between the modes at  $L_{TT}$  equal to zero is caused by the introducing a through hole in the DR. Figure 9 shows the variation of the resonant frequencies as a function of the length of the screws ( $L_{TS}$ ) that are inserted from the side wall of the cavity. The screw diameter was adjusted to 1.5 mm to achieve a proper fit into the gap between the two ceramic pieces. It was observed that the  $EH_{11}^-$  mode was significantly affected

**Table 1.** Comparison of simulated resonance frequency ( $f_r$ ), mode type and  $Q_u$  for the cavity resonator with unpatterned (UNP) and vertically-etched(V-E) structures in triple-mode cavity.

| Mode            | $f_r$ (GHz) |       | $Q_u$ -factor |       | Type   |        |
|-----------------|-------------|-------|---------------|-------|--------|--------|
|                 | UNP         | V-E   | UNP           | V-E   | UNP    | V-E    |
| $EH_{11}$       | 1.96        | 1.989 | 11200         | 11195 | Dual   | Dual   |
| $TE_{01\delta}$ | 1.97        | 2.005 | 7000          | 7585  | single | single |
| $TM_{01}$       | 2.36        | 2.376 | 14700         | 14587 | single | single |

by  $L_{TS}$ , which decreased to about 90 MHz when the  $L_{TS}$  increased by 10 mm. The other modes were minimally affected. This screw is used to provide the required strong inter-resonator coupling between the degenerate  $EH_{11}$  mode.

#### 4. Simulation Result for One Cavity

Figure 10 presents the configuration of the 3<sup>rd</sup> order triple-mode dielectric resonator bandpass filter. The length of the input/output coupling probes  $L_{fh}$ , distance from the centre of DR and hole  $X_r$  are chosen based on the analysis shown in the previous section. Table 2 displays the dimensions of all parameters that affect the coupling.

Figure 11 shows the simulated S-parameters response for a 3<sup>rd</sup> order triple-mode DR filter without any tuning screws. A non-equal ripple of return loss at the inband region was observed and all values are less than 19 dB. The resonant frequency is 2.04 GHz with bandwidth of 56 MHz and maximum insertion loss of about 0.1 dB. The first spurious frequency appeared at 2.426 GHz and the overall suppression window from the resonant frequency is about 382 MHz. Three finite transmission zeros can be observed in the response as follow: a pair of finite transmission zeros occurred at 2.11 GHz and the other is located at 2.318 GHz. The pair of finite transmission zeros are produced by the topology of the triple-mode filter at the resonance frequency, while the final one comes from the spurious band coupling topology.

**Table 2.** Typical dimensions of 3<sup>rd</sup> order filter triple-mode.

| Typical dimensions            |                 | Typical performance              |
|-------------------------------|-----------------|----------------------------------|
| $L_{fh}=18$ mm                | $D_{rh}=5$ mm   | $f_0 = 2.044$ GHz                |
| $W_i = 3$ mm                  | $L_i = 3$ mm    | $\epsilon_r = 43$                |
| T1=4 mm                       | $L_{TS} = 4$ mm | $\tan \delta = 4 \times 10^{-5}$ |
| diameter of $L_{fh} = 2$ mm   |                 | $\sigma = 4 \times 10^7 S/m$     |
| diameter of $L_{TS} = 1.5$ mm |                 |                                  |

Figure 12 shows the simulated S-parameters response of the 3<sup>rd</sup> order filter triple-mode DR with tuning screws. It can be seen that the the in-band ripples were equal and below 22 dB. The resonant frequency and bandwidth were the same as that shown in Figure 11. The second finite transmission zero and first spurious-free frequency were shifted backward by about 28 MHz and 36 MHz respectively, while the pair of finite transmission zeros were shifted upward by about 11 MHz. The extracted Q-factor from the insertion loss and group delay was about 8500. The position of the finite transmission zeros can be moved to the low side of the passband by changing the angle of rotation of the through hole, as shown in Figure 13 and thus enable the possibility of building compact diplexers. Table 3 illustrates the figure-of-merits and extensive comparisons between the novel proposed triple-mode resonator designs and the published research works with the same triple-mode. This design offers a significant improvements based on size and spurious-free window compared with other references.

#### 5. Conclusion

A novel triple-mode dielectric resonator filter has been simulated with finite transmission zeros on the high or low side. It offers a a high Q-factor of 8000, and 15.6%

**Table 3.** Comparison of the proposed triple-mode filter with other references.

| Ref.                      | Resonant frequency (GHz) | Size ( $cm^3$ ) | $Q_u$ | spurious-free window (MHz) | $\epsilon_r$ |
|---------------------------|--------------------------|-----------------|-------|----------------------------|--------------|
| (Wong et al., 2015)       | 2.55                     | 86.4            | 6000  | 230 down/340 up            | 40           |
| (Walker and Hunter, 2002) | 2                        | 260             | 18000 | 500                        | 44           |
| (Hattori et al., 2000)    | 2                        | 112.5           | 12000 | 625                        | 38           |
| This work                 | 2.04                     | 22.7            | 8500  | 387                        | 43           |

volume reduction ratio compared to an air coaxial filter. The gap between the ceramic pieces has a significant effect on the resonant frequency. The filter was operated at the cellular base station specification. Two finite transmission zeros has been generated at the low or high side to improve the out-of-band response.

## References

- Bakr, M. S., Gentili, F., and Bosch, W. (2016a). Triple mode dielectric-loaded cavity band pass filter. In *2016 16th Mediterranean Microwave Symposium (MMS)*, pages 1–3.
- Bakr, M. S., Hunter, I. C., and Bosch, W. (2018a). Miniature triple-mode dielectric resonator filters. In *2018 IEEE/MTT-S International Microwave Symposium - IMS*, pages 1249–1252.
- Bakr, M. S., Hunter, I. C., and Bösch, W. (2018b). Miniature triple-mode dielectric resonator filters. *IEEE Transactions on Microwave Theory and Techniques*, pages 1–7.
- Bakr, M. S., Hunter, I. C., Gentili, F., and Bosch, W. (2016b). A te11dual-mode monoblock dielectric resonator filter. In *2016 Asia-Pacific Microwave Conference (APMC)*, pages 1–4.
- Bakr, M. S., Luhaib, S. W. O., and Hunter, I. C. (2016c). A novel dielectric-loaded dual-mode cavity for cellular base station applications. In *2016 46th European Microwave Conference (EuMC)*, pages 763–766.
- Fiedziuszko, S. J. (1982). Dual-mode dielectric resonator loaded cavity filters. *IEEE Transactions on Microwave Theory and Techniques*, 30(9):1311–1316.
- Hattori, J., Wakamatsu, H., Kubo, H., and Ishikawa, Y. (2000). 2 GHz band triple mode dielectric resonator duplexer for digital cellular base station. In *Microwave Conference, 2000 Asia-Pacific*, pages 1315–1318. IEEE.
- Hong, J. S. (2000). Couplings of asynchronously tuned coupled microwave resonators. *IEE Proceedings - Microwaves, Antennas and Propagation*, 147(5):354–358.
- Hunter, I. C., Billonet, L., Jarry, B., and Guillon, P. (2002). Microwave filters-applications and technology. *IEEE Transactions on Microwave Theory and Techniques*, 50(3):794–805.
- Liang, J.-F. and Blair, W. D. (1998). High-q te01 mode dr filters for pcs wireless base stations. *IEEE Transactions on Microwave Theory and Techniques*, 46(12):2493–2500.
- Luhaib, S., Somjit, N., and Hunter, I. C. (2018). Improvement of the stopband spurious window for a dual-mode dielectric resonator filter by new coupling technique. *International Journal of Electronics*, (just-accepted).
- Walker, V. and Hunter, I. C. (2002). Design of triple mode TE<sub>01δ</sub> resonator transmission filters. *IEEE Microwave and wireless components letters*, 12(6):215–217.
- Wong, S.-W., Zhang, Z.-C., Feng, S.-F., Chen, F.-C., Zhu, L., and Chu, Q.-X. (2015). Triple-mode dielectric resonator duplexer for base-station applications. *IEEE Transactions on Microwave Theory and Techniques*, 63(12):3947–3953.

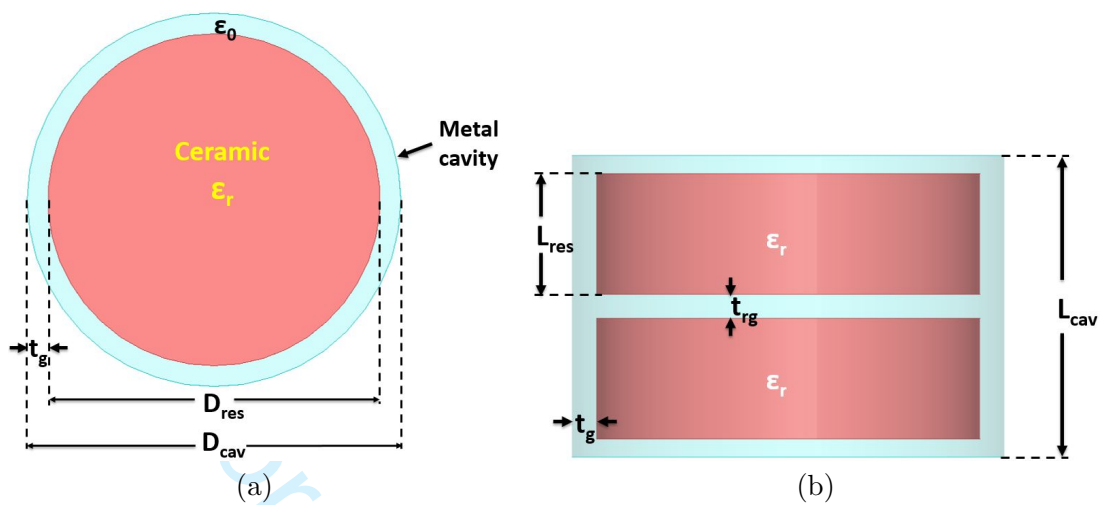


Figure 1. Configuration of triple-mode DR (a) Top view, (b) Side view.

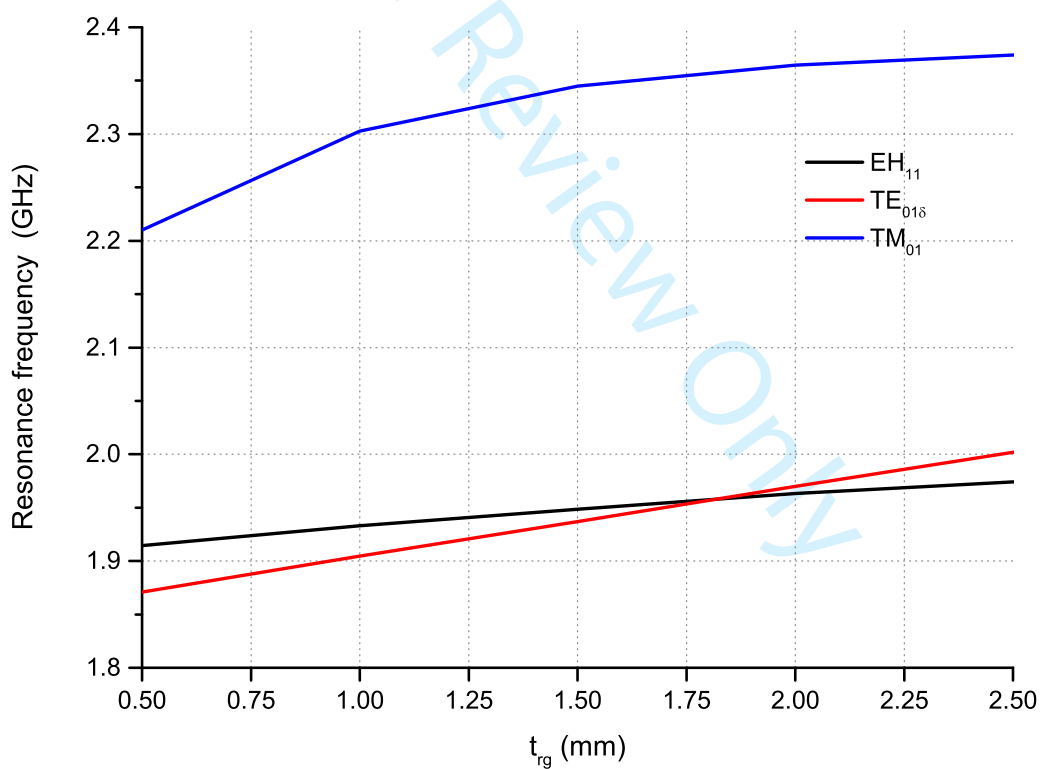
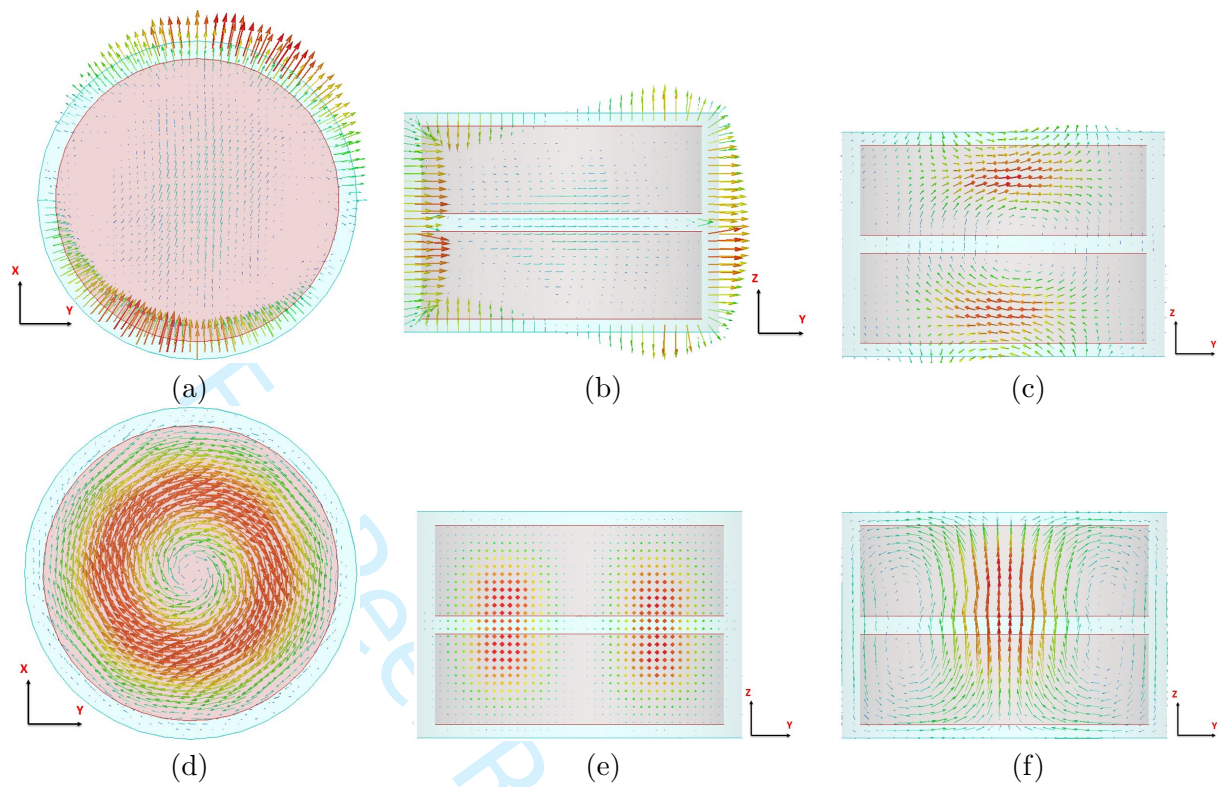
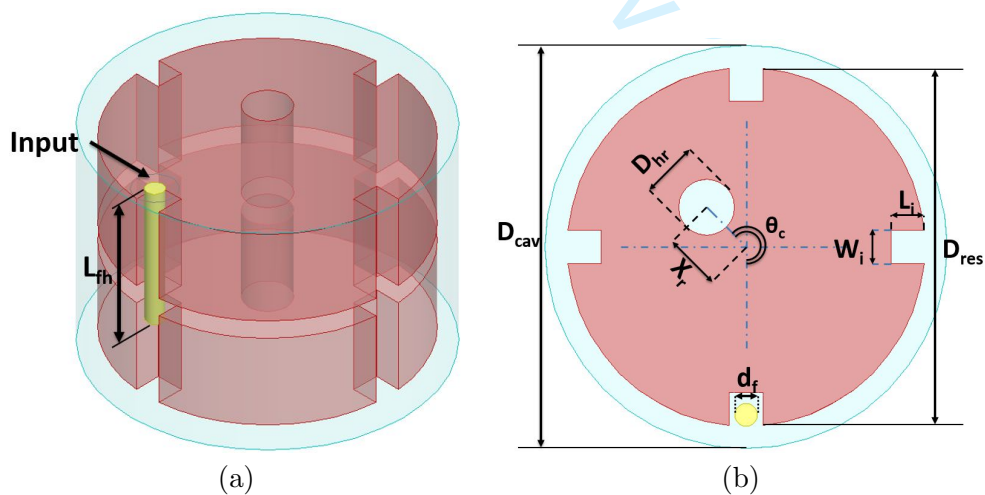


Figure 2. Resonant frequencies against  $t_{rg}$ .



**Figure 3.** E and H field pattern (a) and (b) E-field for  $EH_{11}$  (c) H-field for  $EH_{11}$  (d) and (e) E-field for  $TE_{01\delta}$  (f) H-field for  $TE_{01\delta}$ .



**Figure 4.** I/O and inter-resonator coupling for triple-mode cavity (a) 3D view (b) top view.

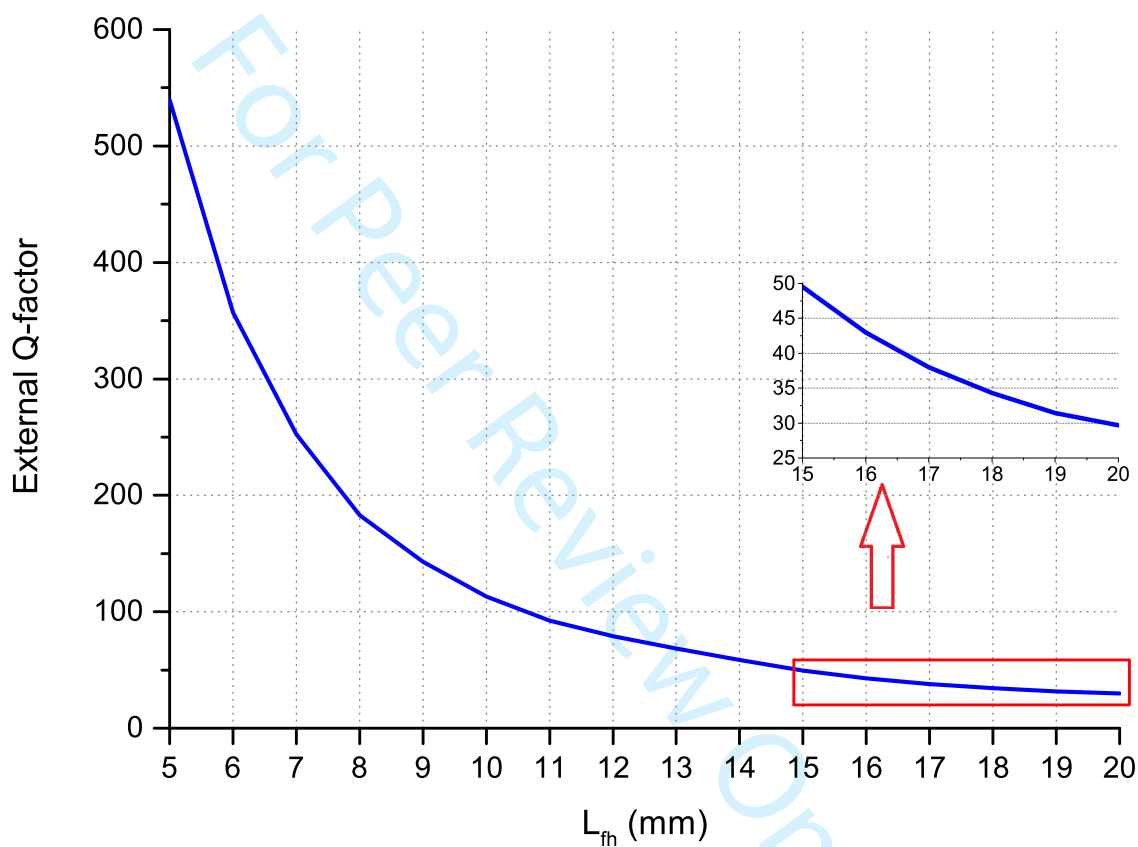


Figure 5. External Q-factor varying with length of I/O coupling probe.

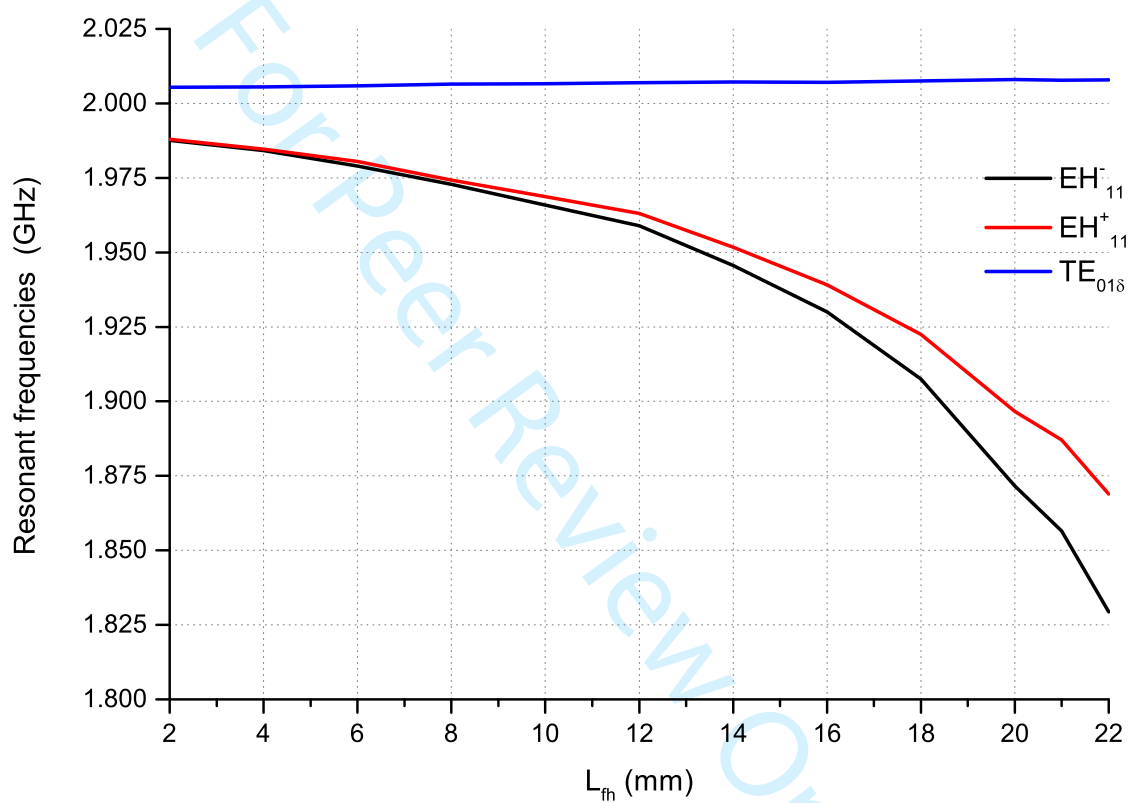


Figure 6. Resonant frequencies varying with length of I/O coupling probe.

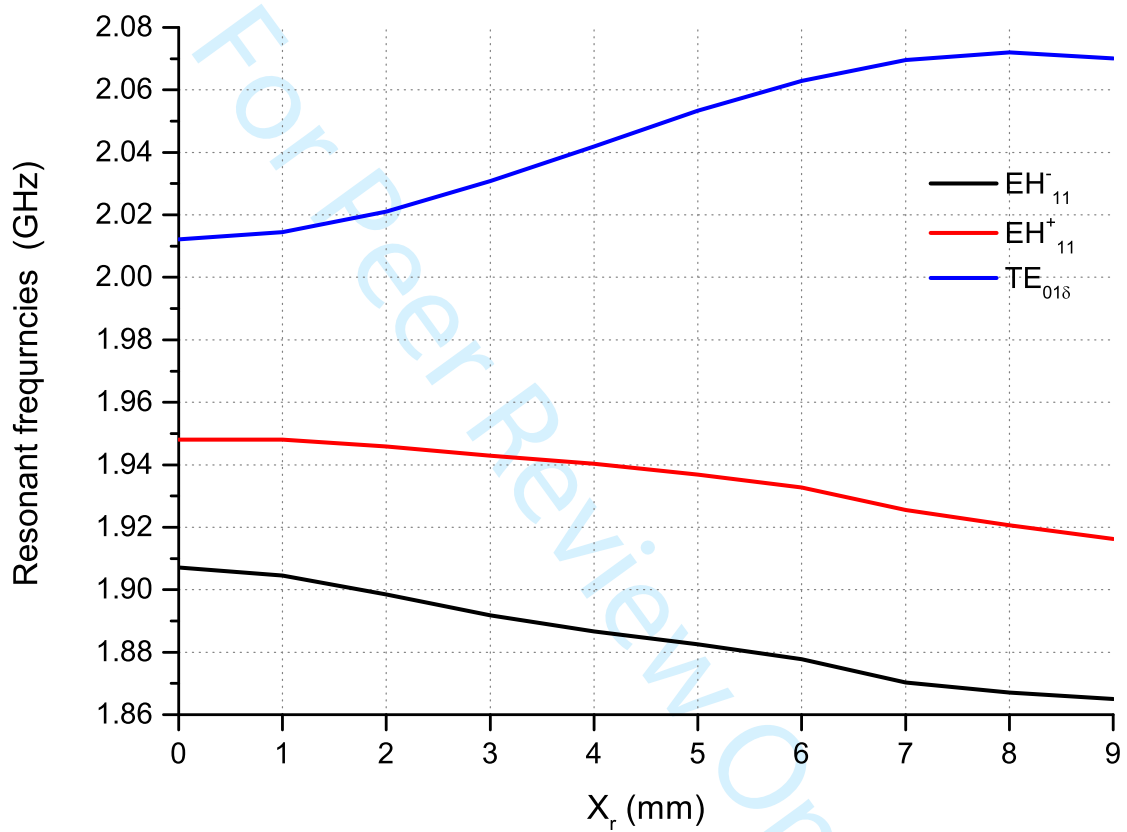


Figure 7. Resonant frequencies varying with offset of hole ( $X_r$ ).

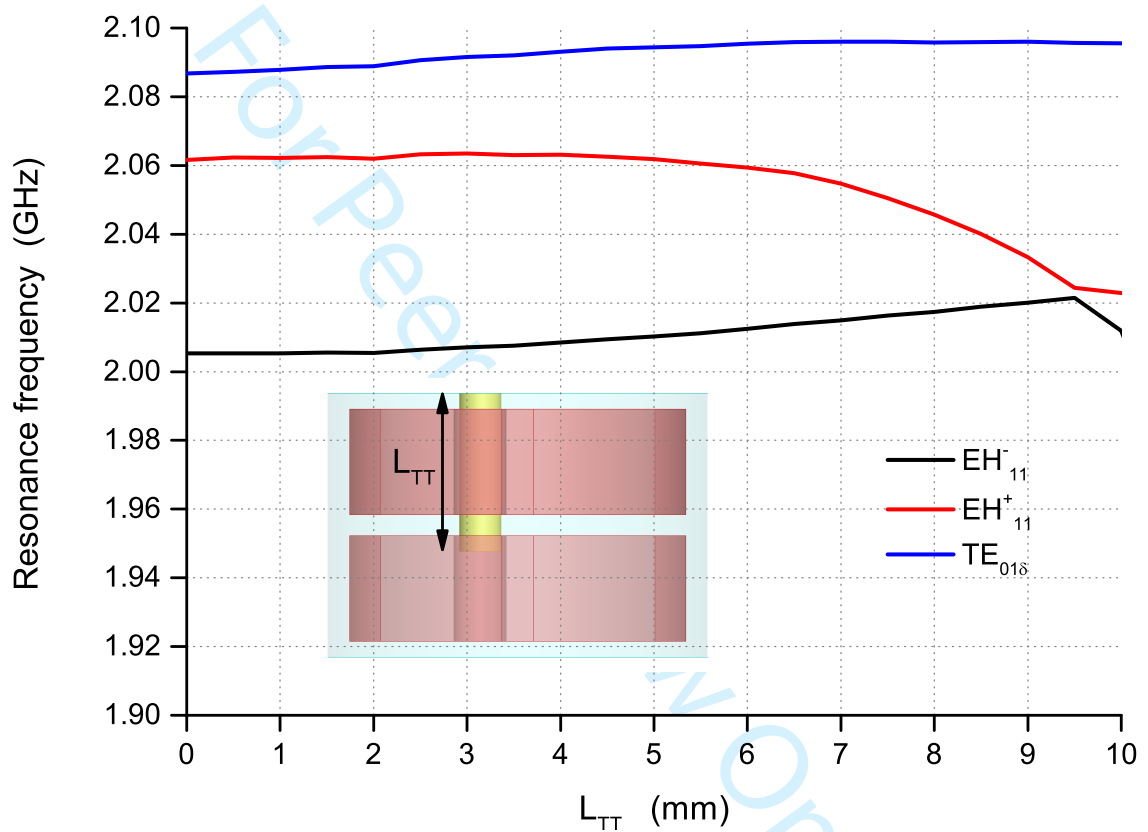


Figure 8. Resonant frequencies varying with  $L_{TT}$ .

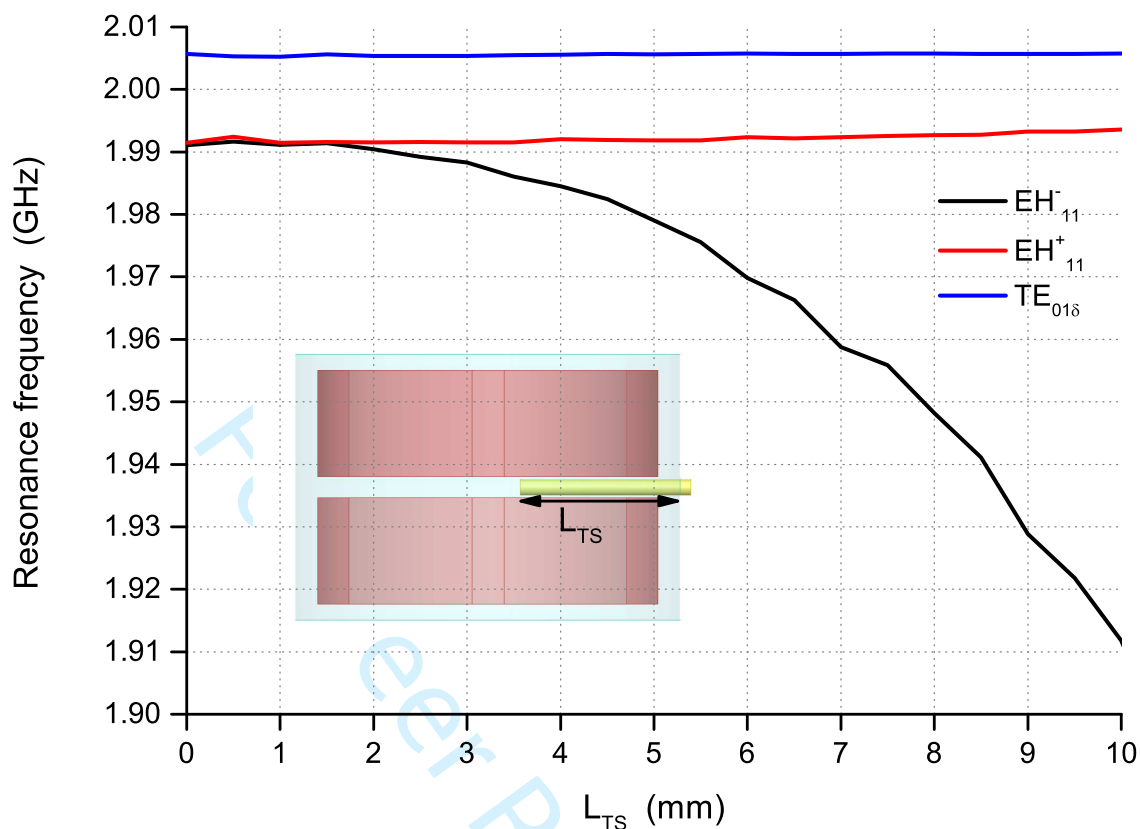


Figure 9. Resonant frequencies varying against  $L_{TS}$ .

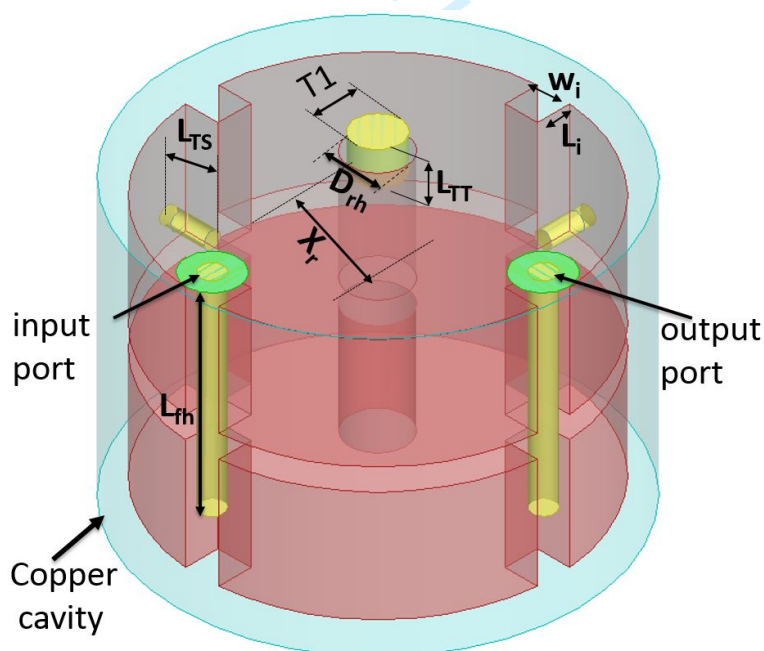


Figure 10. Structure of triple-mode 3<sup>rd</sup> order filter in HFSS.

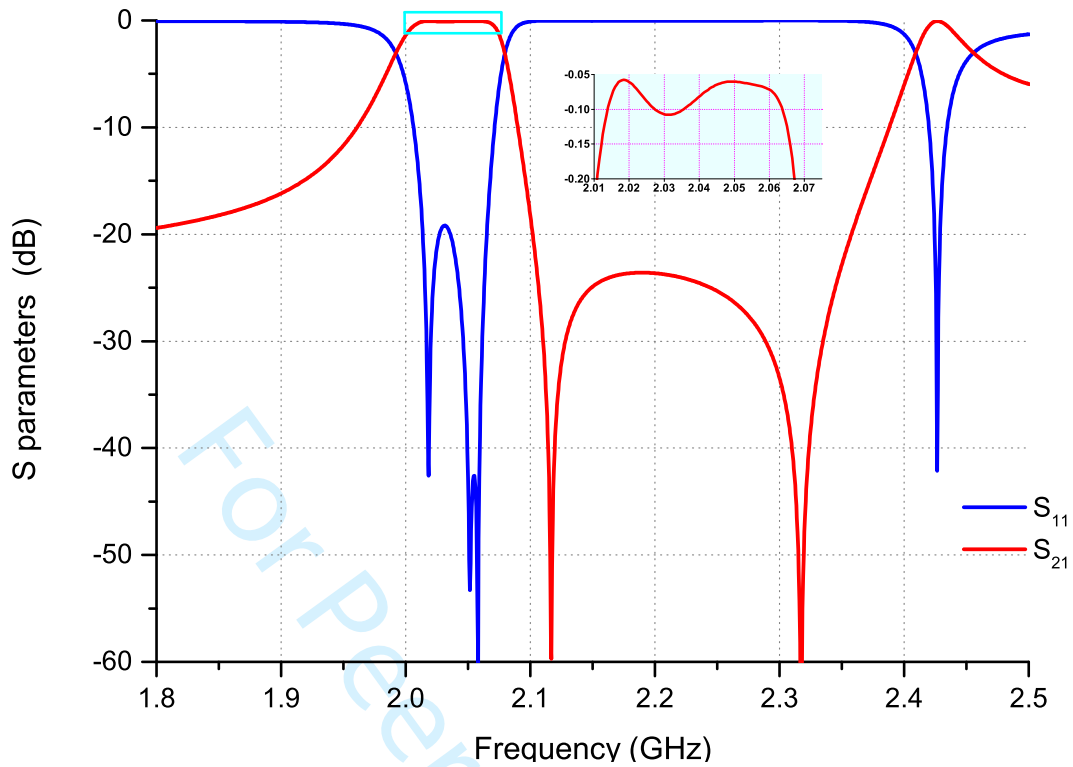


Figure 11. Frequency response of triple-mode filter without tuning screws.

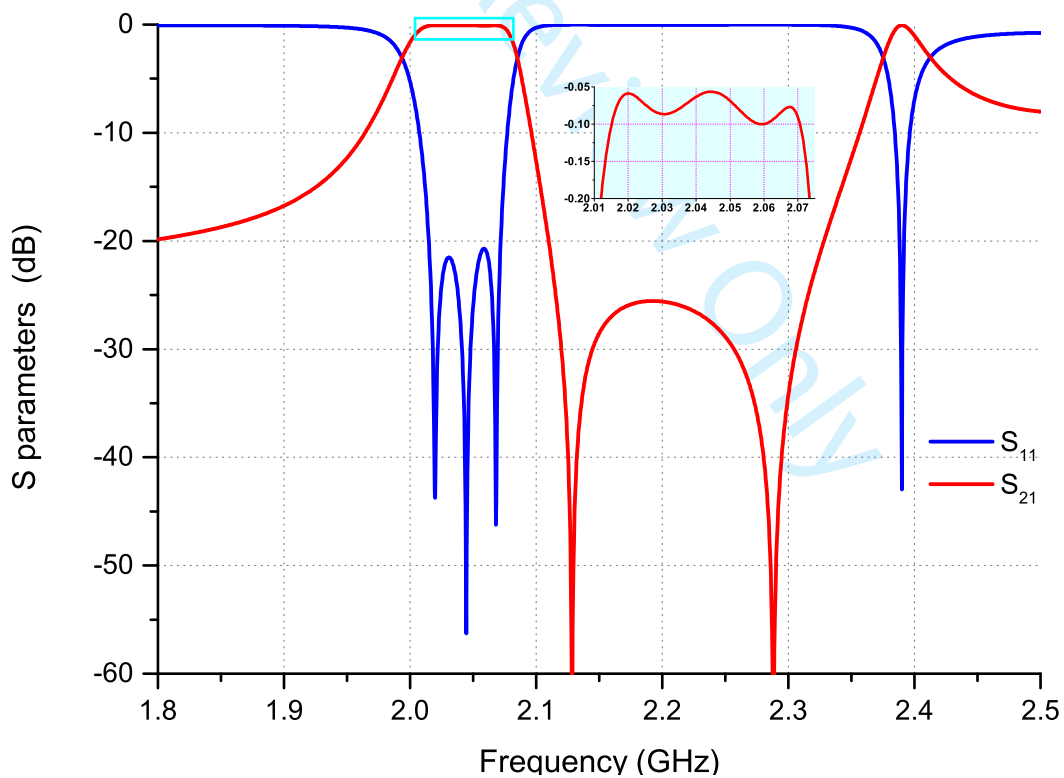


Figure 12. Frequency response of triple-mode filter with tuning screws.

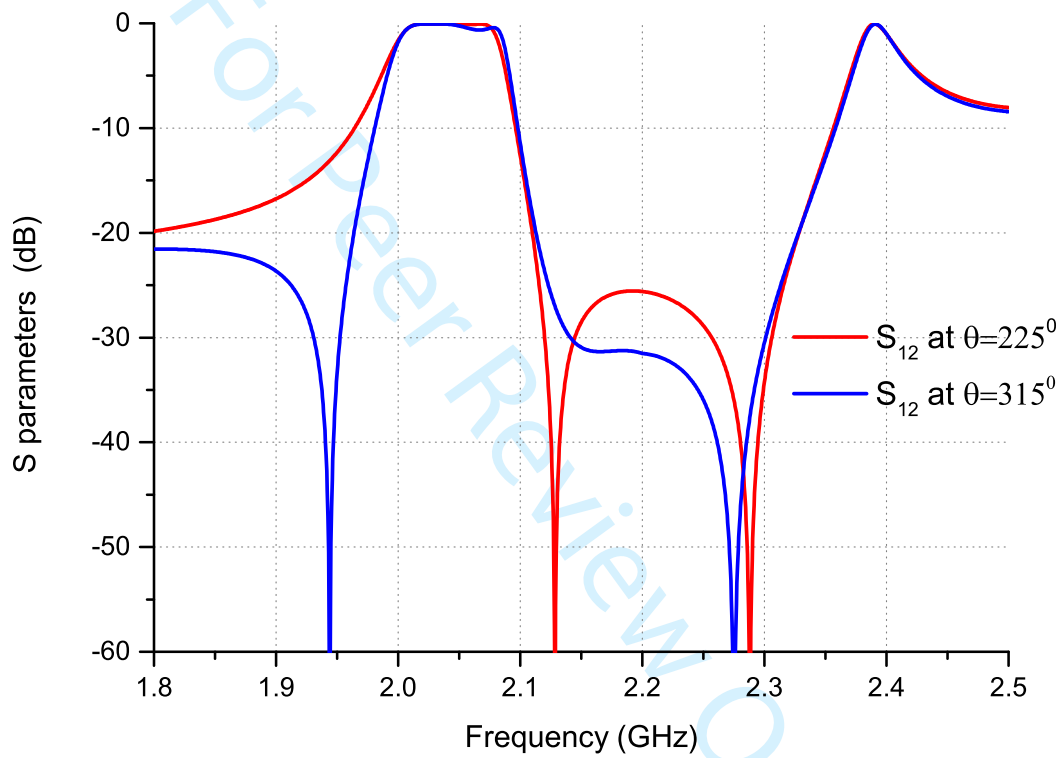


Figure 13. Frequency response of triple-mode filter at  $\theta_c = 315^\circ$  and  $\theta_c = 215^\circ$ .